The International Journal of Engineering And Science (IJES)
||Volume|| 2 ||Issue|| 1 ||Pages|| 85-92 ||2013||
ISSN: 2319 – 1813 ISBN: 2319 – 1805

Mimo-Ofdm Systems with Papr Reduction and Ici Canceller

[1]P.Sasikala, [2]Dr. T.Pearson
[1] *M.E (Communication systems), Anna University*
[2]*DEAN-ECE, DMI College of Engineering*

----------Abstract----------

In this paper, efficient method for ICI cancellation based on factor graph and PAPR reduction using precoder by estimating CFO and channel parameters in MIMO-OFDM based wireless communication systems is proposed. By exchanging messages both in space domain and frequency domain, the proposed algorithm can suppress ICI and reduce PAPR iteratively and progressively. The performances of PPIC, both in perfect channel estimation and imperfect channel estimation cases, are compared with the standard PIC architecture and the ICI self-canceller. The joint scheme of CFO and channel estimation in the MIMO-OFDM systems with the MSE based precoder for reducing PAPR. First, a MSE based precoding matrix to reduce the PAPR of OFDM signals is designed. The CFO and CIR estimators based on the EM algorithm with an iterative scheme are developed to execute the estimations. To reduce computational complexity, a simpler coarse CFO estimator is carried out before the fine estimation so that a more accurate and faster convergent estimate can be attained. It is very suitable for VLSI implementation and it is a potential candidate for data detection/decoding in future high data rate, high mobility wireless communication systems.

Key words- *EM algorithm, factor graph, ICI cancellation, MIMO-OFDM, PAPR.*

Date of Submission: 19, December, 2012 ⟺ Date of Publication: 05, January 2013

I. Introduction

Orthogonal frequency division multiplexing (OFDM) is a popular method for high data rate wireless transmission. MIMO systems resort to antenna diversity to achieve the additional extraordinary throughput or reliability without additional power consumption. In order to combat the multi-path delay spread, one efficient method in MIMO is to take advantage of the orthogonal frequency-division multiplexing (OFDM), which transforms a multi-path fading channel to parallel independent flat-fading sub-channels. Moreover, the sub-carriers in OFDM system are overlapping to maximize spectral efficiency. Therefore, the combination of MIMO and OFDM has got much attention in recent wireless communication researches. Despite the advantage of MIMO-OFDM is very attractive, there are some technical problems need to overcome. MIMO-OFDM faces two major challenges. First, just like the single antenna OFDM system, MIMO-OFDM is very sensitive to the CFO caused by oscillator mismatches or Doppler shifts between the transmitter and receiver. The second challenge of MIMO-OFDM is that the multi-path channel estimation becomes more difficult with the increase of the number of antennas. In order to take advantage of the MIMO scheme, the knowledge of precise CSI is required.This paper focus on the joint estimation of CFO and CIR in MIMO-OFDM systems with the PAPR reduction precoding matrix. In general, applying the maximum likelihood method to the combined estimation of CFO and CIR usually leads to the problems of high complexity. Thus, we resort to the expectation-maximization (EM) algorithm and derive an iterative scheme to overcome this difficulty. In view of computational complexity, the estimation process divided into the coarse and fine estimation phases. A coarse CFO estimator is derived to evaluate an initiate estimate. Then the fine estimation is performed by making use of the EM iteration algorithm. Finally, the simulations of the proposed estimators are performed and the results are evaluated.

In a MIMO system, as data are transmitted/received through different antennas, many channel impairments need to be dealt with, such as multipath fading, AWGN noise, inter-antenna interference etc. To effectively deal with these channel impairments, many types of MIMO detectors such as MAP detector [1], sphere decoder [2], MMSE-SIC detector [1], [3], etc. have been proposed. For OFDM-based systems, the transmission bandwidth is divided into many narrow subchannels, which are transmitted in parallel. As a result, the symbol duration is increased and the intersymbol interference (ISI) caused by a multipath fading channel is alleviated. However, with longer symbol duration, channel's time variations lead to a loss of subchannel orthogonality, known as inter-carrier interference (ICI). As delay spread increases, symbol duration should also increase in order to maintain a nearly flat channel in every frequency subband. Also due to high demand for bandwidth, there is a trend toward using higher frequency bands.

In recent years, ICI cancellation has received considerable attention. In [4], [7], [8], the performance degradation due to ICI is analyzed. It is shown that ICI can be modeled as an additive near-Gaussian random process that leads to an error floor which depends on the normalized Doppler frequency. In [9] and [10], the well-known ICI self-cancellation scheme is proposed. By appropriately mapping symbols to a group of subcarriers, the proposed algorithm in [9] makes OFDM transmissions less sensitive to the ICI at the cost of much lower bandwidth efficiency. The message passing data detector/decoder catches the attention of many researchers. One appealing practical aspect of the message passing data detector/decoder is due to that it consists of much small, independent detection/decoding functions to deal with channel impairments. Hardware could be implemented according to these independent detectors/decoders and operated in parallel, and it potentially leads to a very-high-speed detector/decoder. This aspect is particularly important in data transmissions where data rate requirements are high, and processing delay must be low.

Based on factor graph, a joint design of a message passing MIMO data detector/decoder with a progressive parallel intercarrier interference canceller (PPIC) for OFDM-based wireless communication systems is proposed in this paper. The message type chosen in this work is log-likelihood ratio (LLR) of bit probabilities for the MIMO data detector/decoder and soft data symbols for the PPIC ICI canceller. The proposed algorithm detects the transmitted data iteratively, by jointly dealing with channel fading effects, AWGN noise and interferences in time domain, frequency domain and space domain. With the insertion of cyclic prefix, the time domain ISI can be avoided. With the message passing MIMO detector (denoted as MPD in the following sections), the space domain inter antenna interference can be suppressed and with the aid of PPIC, the frequency domain ICI can be cancelled. Besides, the computational complexity of the proposed PPIC architecture is relatively lower than the standard PIC architecture.

II. Mimo-Ofdm Systems With Precoder

System Description (Figure 1) Consider an N_t transmit antenna, N_r receive antenna MIMO-OFDM system with precoding for PAPR reduction, and suppose that the subcarriers over the channel suffer from a CFO. At the transmitting end, input data are fIrst modulated by M -ary phase shift keying (PSK) mapping. Each modulated signal vector $U_j[n]$ at the time index n is encoded by the precoder P before the IFFT transform for j =1 , . . . , N_t , as shown in Fig.I (a). The precoding matrix P is chosen for PAPR reduction with the minimum error probability and is defined as follows

$$:P=[b_0^T \;\; b_1^T \;\; \dots \;\; b_{M-1}^T]^T_{MXN}, \quad \text{.....(1)}$$

where $(\cdot)^T$ denotes the transpose operation and $b_k^T = C_k[1, \exp(-2\pi k/N), \dots, \exp(-2\pi(N-1)/N)]_{1XN}$ with C_k , k = 0, ... , M - 1 , the Fourier coefficients of the chosen pulse shape. After the precoding process, the signal vector can be expressed as

$$:X_j=PU_j[n], \quad j=1\dots N_t, \dots\dots (2)$$

Where Xj[m] = $[X_j^0, X_j^1, \dots, X_j^{N-1}]$T denotes the m -th transmitted symbol from the j -th transmit antenna, and X_j^kdenotes the signal corresponding to the k -th subcarrier. After the Inverse Fast Fourier Transform (IFFT) process, the time domain signal xj[m] can be expressed as

$$:X_j[m] = F^H \cdot X_j[m], \quad \ldots\ldots (3)$$

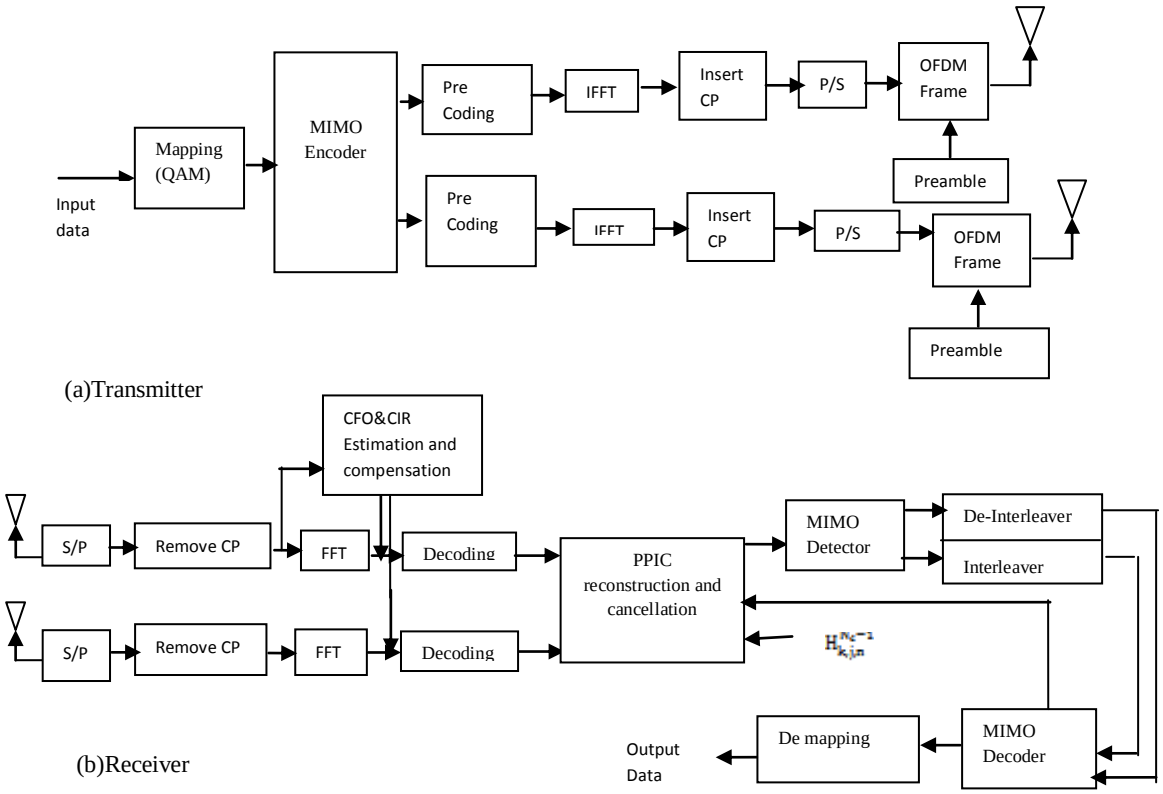

Fig: 1 Block Diagram of MIMO-OFDM System (a) Transmitter (b) Receiver

Where the symbol $(\cdot)^H$ denotes the Hermitian transpose and F is the N -point IFFT matrix defIned as,

$$:F^H = \begin{bmatrix} W_N^{-00} & W_N^{-01} \ldots & W_N^{-0(N-1)} \\ W_N^{-10} & W_N^{-11} & \vdots \\ \vdots & \vdots & \vdots \\ W_N^{-(N-1)0} & W_N^{-(N-1)0} & W_N^{-(N-1)(N-1)} \end{bmatrix}, \quad \ldots\ldots (4)$$

$$\textbf{Where,} \qquad :W_N = \frac{1}{\sqrt{N}} e^{-\frac{j2\pi}{N}} \quad \ldots\ldots(5)$$

The data transmission unit is carried out in the frame (burst) mode. Each frame consists of D +1 OFDM blocks. The fIrst block, also called preamble, comprise training sequence for performing the estimation of CFO and CIR. The remaining blocks D are the data symbols of OFDM. The following description will focus on the preamble block. Here we suppose that the fading processes associated with different antenna pairs are uncorrelated and remain static during each block but vary from one OFDM block to another and that the CP length is longer than or equal to the maximum channel delay spread. All antenna pairs are assumed to be affected by the same CFO.

III. Estimation Of Cfo And Channel Impulse Response

According to (8), the channel impulse response (CIR) h_i conditioned on y_i and ε is complex Gaussian distributed [9] with $h_i \mid (y_i, \varepsilon) \sim CN(\hat{h}_i, \hat{\sum}_{hi})$. Where $\hat{h}_i$ and $\hat{\sum}_{hi}$ denote, respectively, the mean vector and covariance matrix of the channel response h_i. By applying the linear minimum mean square error estimation (LMMSE) [9], the channel conditional mean $\hat{h}_i$ becomes

$$:\hat{h}_i = E[h_i \mid (y_i, \varepsilon)] = \hat{\sum}_{hi} D^H \Gamma^H(\varepsilon) \sum_{vi}^{-1} y_i, \quad \ldots..(6)$$

$$:\hat{\sum}_{hi} = (D^H \Gamma^H(\varepsilon) \sum_{vi}^{-1} \Gamma(\varepsilon) D + \sum_{hi}^{\perp})^{-1}, \quad \ldots..(7)$$

Where $\sum_{hi} = E(h_i h_i^H) = diag\{\sigma_{i,j,0}^2, \sigma_{i,j,1}^2, \ldots, \sigma_{i,j,L-1}^2, \ldots, \sigma_{i,j,0}^2, \sigma_{i,Nt-1}^2, \ldots, \sigma_{i,Nt,L-1}^2\}$ with

$\sigma^2_{i,j,l}$ the average power of the l th tap between the j –th transmit antenna and the i-th received antenna.

If the channel response at this tap is zero, we have $\sigma^2_{i,j,l}$=0. The diagonal elements of D^HD are equal to N/N_t, Which in general is much larger than $\sigma^2_{vi}/\sigma^2_{i,j,l}$. Thus, an approximate expression of CIR can be obtained as

$$:\hat{\mathbf{h}}_i \approx (\mathbf{D}^H\mathbf{D})^{-1}\mathbf{D}^H\,\Gamma(\varepsilon^{(k)})\mathbf{y}_i, \quad .....(8)$$

3.1 The CFO estimator

The likelihood function based on the signal model in [7] to yield

$$:A(\varepsilon, \mathbf{h}_i|\mathbf{y}_i) = \frac{1}{(\pi\sigma^2_{vi})^N}\exp\{-\frac{1}{\sigma^2_{vi}}\|\mathbf{y}_i - \Gamma(\varepsilon)\mathbf{D}\mathbf{h}_i\|^2\}, \quad .....(9)$$

The EM based algorithm is used here to obtain an estimate of CFO that consists of the following two steps

(1) E-step:

$$:Q(\varepsilon|\varepsilon^{(k)}) = E\{[\sum_{i=1}^{Nr}\log\Lambda_i(\varepsilon,\mathbf{h}_i|\mathbf{y}_i)]|\mathbf{y}_i,\varepsilon^k\}, \quad .....(10)$$

(2) M-step:

$$:\varepsilon^{(k+1)} = \arg\max_{\varepsilon} Q(\varepsilon|\varepsilon^{(k)}), \quad .....(11)$$

In the E-step, the expectation is taken with respect to the hidden channel response $\hat{h}_i$ conditioned on y_i and ε. Hence, E-step equation reduces to

$$:Q(\varepsilon|\varepsilon^{(k)}) = \sum_{i=1}^{Nr}\mathrm{Re}(\mathbf{y}_i\,\Gamma(\varepsilon)\mathbf{D}\hat{\mathbf{h}}_i^{(k)}), \quad .....(12)$$

In the M-step, which is used for computing the (k+1)-th estimate of ε, can be represented by

$$:\varepsilon^{(k+1)} = \arg\max_{\varepsilon}\sum_{i=1}^{Nr}\mathrm{Re}(\mathbf{y}_i\,\Gamma(\varepsilon)\mathbf{D}\hat{\mathbf{h}}_i^{(k)}), \quad .....(13)$$

Which is defined as the CFOE#1 estimator. After the first EM procedure is done,we use this new estimate to update the channel estimator in (11).Then repeat the EM process until the estimate converges.

3.2The coarse CFO estimator

The EM algorithm is a robust process. However its computational complexity will increase with the amount of subcarriers and a range of the frequency offsets. To reduce the complexity by making use of a simple transform and some assumptions. The Taylor series expansion of an exponential function will be introduced in this subsection. By defining the NX1 vector $G_i^{(k)}$=D $\hat{\mathbf{h}}_i^{(k)}$,so

$$:\varepsilon^{(k+1)} = \arg\max_{\varepsilon}\left\{Re\left(\sum_{i=1}^{Nr}\sum_{n=0}^{N-1}\mathbf{y}_i^*(\mathbf{n})\,G_i^{(k)}(\mathbf{n})\exp\left(\frac{j2\pi\varepsilon n}{N}\right)\right)\right\}, \quad .....(14)$$

Where $(\cdot)^*$ denotes the conjucate operation. The exponential term exp(j2πεn/N) in above equation is expanded into the Taylor series. With the assumption of a small ε, take only the first two terms of the series as the approximation.

$$:\exp\left(\frac{j2\pi\varepsilon n}{N}\right) = 1+\left(\frac{j2\pi n}{N}\right)\varepsilon-\left(\frac{j2\pi n}{N}\right)\varepsilon^2, \quad .....(15)$$

Hence the likelihood function Q ($\varepsilon|\varepsilon^{(k)}$) becomes the quadratic function of $\varepsilon^{(k)}$. By taking the first order derivative with respect to ε and setting it equal to zero, an optimum solution (the CFOE#2 estimator) is obtained as follows

$$:\varepsilon^{(k+1)} = -\frac{N}{2\pi}\frac{\sum_{i=1}^{Nr}\sum_{n=0}^{N-1}n\,Im\{\mathbf{y}_i^*(\mathbf{n})\,G_i^{(k)}(\mathbf{n})\}}{\sum_{i=1}^{Nr}\sum_{n=0}^{N-1}\mathbf{n}^2\mathrm{Re}\{\mathbf{y}_i^*(\mathbf{n})\,G_i^{(k)}(\mathbf{n})\}}, \quad .....(16)$$

IV. Progressive Pic Architecture

The PPIC architecture is modeled as a factor graph. The subcarrier nodes represented as blocks for ICI cancellation execute the function of interference reconstruction and cancellation. The message type is soft data symbol. The estimated soft data symbols are exchanged between adjacent subcarrier nodes and stored. At the 1st iteration, the nth subcarrier node receives and stores the soft symbols from the (n+1)h subcarrier node and the (n−1)th subcarrier node. These soft data symbols are used for ICI reconstruction and cancellation. So, the ICI from the (n+1)h subcarrier and the (n − 1)th subcarrier are reconstructed and cancelled. At

the 2*nd* iteration, the *nth* subcarrier node receives and stores the soft symbols, which are estimated at the 2*nd* iteration, from the $(n+1)h$ subcarrier node and the $(n-1)th$ subcarrier node, and the soft symbols, which are stored at the 1*st* iteration, from the $(n+1)th$ subcarrier node and the $(n-1)th$ subcarrier node. These stored data symbols are actually estimated by the $(n+2)h$ subcarrier node and the $(n-2)th$ subcarrier node at the 1*st* iteration. So, the ICI from the $(n+1)h$ subcarrier, $(n+2)th$ subcarrier, $(n-1)th$ subcarrier and $(n-2)th$ subcarrier are reconstructed and cancelled. In this way, the ICI are reconstructed and cancelled iteratively and progressively from the received signal. At the 1st iteration, the two strongest interfering subcarriers are cancelled. At the 2*nd* iteration, the two strongest and the two adjacent less strong interfering subcarriers are cancelled. At the *ith* iteration, the ICI from 2*i* adjacent subcarriers are cancelled. Stated more formally, at the $0th$ iteration, the estimated soft data symbols for the *jth* transmit antenna and the reconstructed ICI at the *kth* receive antenna are initialized to **0**:

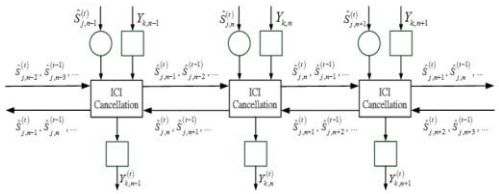

Fig: 2 **Factor** graph of the PPIC architecture

$$:\hat{S}_{j}^{(0)} = \left[\cdots\ \hat{S}_{j,n-1}^{(0)}\ \hat{S}_{j,n}^{(0)}\ \hat{S}_{j,n+1}^{(0)}\ \cdots\right] = \mathbf{0}\ ,\quad \textbf{..(17)}$$

$$:\hat{S}_{ICI,k}^{(0)} = \left[\cdots\ \hat{S}_{ICI,k,n-1}^{(0)}\ \hat{S}_{ICI,k,n}^{(0)}\ \hat{S}_{ICI,k,n+1}^{(0)}\ \cdots\right] = \mathbf{0},\quad \textbf{.....(18)}$$

Hence, the ICI cancelled signals are exactly the same as the received signals:

$$:Y_{k}^{(0)} = Y_{k} - \hat{S}_{ICI,k}^{(0)} = Y_{k}\ ,\quad \textbf{.....(19)}$$

The results are fed forward to the MPD and LDPC decoder as described in previous section to be further processed. At the 1 *st* iteration, the estimated soft data symbols are fed back from the LDPC decoder. These soft data symbols are exchanged between adjacent subcarrier nodes and stored. Take the *nth* subcarrier node for example, it receives and stores:

$$:\hat{S}_{j,n}^{(1)} = \left[\hat{S}_{j,((n-1))N_c}^{(1)}\ \hat{S}_{j,((n+1))N_c}^{(1)}\right],\quad \textbf{..... (20)}$$

According the results in (19), The ICI from the $(n+1)h$ subcarrier and the $(n-1)th$ subcarrier are reconstructed and cancelled.

$$:\hat{S}_{ICI,k,n}^{(1)} = H_{k,j,n}^{1}\cdot\hat{S}_{j,((n-1))N_c}^{(1)} + H_{k,j,n}^{N_c-1}\cdot\hat{S}_{j,((n+1))N_c}^{(1)}\ ,\quad \textbf{.....(21)}$$

$$:Y_{k}^{(1)} = Y_{k} - \hat{S}_{ICI,k}^{(1)}\ ,\quad \textbf{..... (22)}$$

Afterwards, data are detected by the MPD and LDPC decoder. At the 2 *nd* iteration, the processes in the 1 *st* iteration are repeated. The n *th* subcarrier node receives and stores

$$:\hat{S}_{j,n}^{(2)} = \begin{bmatrix}\hat{S}_{j,((n-2))N_c}^{(1)} & \hat{S}_{j,((n-1))N_c}^{(2)}\\ \hat{S}_{j,((n+1))N_c}^{(2)} & \hat{S}_{j,((n+2))N_c}^{(1)}\end{bmatrix},\quad \textbf{..... (23)}$$

So, the ICI from the (n+1)*th* subcarrier, (n+2)*th* subcarrier, (n-1)*th* subcarrier and (n-2)*th* subcarrier are reconstructed and cancelled

$$:\hat{S}_{ICI,k,n}^{(2)} = H_{k,j,n}^{1}\cdot\hat{S}_{j,((n-1))N_c}^{(2)} + H_{k,j,n}^{2}\cdot\hat{S}_{j,((n-2))N_c}^{(1)} + H_{k,j,n}^{N_c-2}\cdot\hat{S}_{j,((n+2))N_c}^{(1)} + H_{k,j,n}^{N_c-1}\cdot\hat{S}_{j,((n+1))N_c}^{(2)}\ ,\quad \textbf{.....(24)}$$

$$:Y_{k}^{(2)} = Y_{k} - \hat{S}_{ICI,k}^{(2)}\ ,\quad \textbf{.....(25)}$$

At the t *th* iteration, the soft data symbols from the adjacent 2t subcarriers are received and stored by the n *th* subcarrier node:

$$:\hat{S}_{j,n}^{(t)} = \begin{bmatrix}\hat{S}_{j,((n-t))N_c}^{(1)} & \cdots & \hat{S}_{j,((n-2))N_c}^{(t-1)} & \hat{S}_{j,((n-1))N_c}^{(t)}\\ \hat{S}_{j,((n+1))N_c}^{(t)} & \hat{S}_{j,((n+2))N_c}^{(t-1)} & \cdots & \hat{S}_{j,((n+t))N_c}^{(1)}\end{bmatrix},\quad \textbf{.....(26)}$$

The ICI from the adjacent 2t subcarriers can be reconstructed and cancelled:

$$:\hat{S}_{ICI,k,n}^{(t)} = H_{k,j,n}^{1}\cdot\hat{S}_{j,((n-1))N_c}^{(t)} + H_{k,j,n}^{2}\cdot\hat{S}_{j,((n-2))N_c}^{(t-1)} + \cdots + H_{k,j,n}^{t}\cdot\hat{S}_{j,((n-t))N_c}^{(1)} + H_{k,j,n}^{N_c-t}\cdot\hat{S}_{j,((n+2))N_c}^{(1)} + \cdots + H_{k,j,n}^{N_c-2}\cdot\hat{S}_{j,((n+2))N_c}^{(t-1)} + H_{k,j,n}^{N_c-1}\cdot\hat{S}_{j,((n+1))N_c}^{(t)}\ ,\quad \textbf{..... (27)}$$

So that,

$$: \mathbf{Y}_{\mathbf{k}}^{(t)} = \mathbf{Y}_{\mathbf{k}} - \hat{\mathbf{S}}_{\mathbf{ICI},\mathbf{k}}^{(t)}, \quad \ldots\ldots \textbf{(28)}$$

Furthermore, each column of the channel matrix $H_{k,j}$ as shown below is calculated only when it is needed. In the 0^{th} iteration, $H_{k,j}^{0} = [H_{k,j,0}^{0} \cdots H_{k,j,N_c-1}^{0}]^T$ needs to be calculated. In the 1 *st* iteration,

$$: \mathbf{H}_{\mathbf{k,j}} = \begin{bmatrix} \mathbf{H}_{\mathbf{k,j,0}}^{\mathbf{0}} & \mathbf{H}_{\mathbf{k,j,0}}^{\mathbf{1}} & \mathbf{H}_{\mathbf{k,j,0}}^{\mathbf{2}} & \cdots & \mathbf{H}_{\mathbf{k,j,0}}^{\mathbf{N_c-2}} & \mathbf{H}_{\mathbf{k,j,0}}^{\mathbf{N_c-1}} \\ \mathbf{H}_{\mathbf{k,j,1}}^{\mathbf{0}} & \mathbf{H}_{\mathbf{k,j,1}}^{\mathbf{1}} & \mathbf{H}_{\mathbf{k,j,1}}^{\mathbf{2}} & \cdots & \mathbf{H}_{\mathbf{k,j,1}}^{\mathbf{N_c-2}} & \mathbf{H}_{\mathbf{k,j,1}}^{\mathbf{N_c-1}} \\ \vdots & \vdots & \vdots & \ddots & \vdots & \vdots \\ \mathbf{H}_{\mathbf{k,j,N_c-2}}^{\mathbf{0}} & \mathbf{H}_{\mathbf{k,j,N_c-2}}^{\mathbf{1}} & \mathbf{H}_{\mathbf{k,j,N_c-2}}^{\mathbf{2}} & \cdots & \mathbf{H}_{\mathbf{k,j,N_c-2}}^{\mathbf{N_c-2}} & \mathbf{H}_{\mathbf{k,j,N_c-2}}^{\mathbf{N_c-1}} \\ \mathbf{H}_{\mathbf{k,j,N_c-1}}^{\mathbf{0}} & \mathbf{H}_{\mathbf{k,j,N_c-1}}^{\mathbf{1}} & \mathbf{H}_{\mathbf{k,j,N_c-1}}^{\mathbf{2}} & \cdots & \mathbf{H}_{\mathbf{k,j,N_c-1}}^{\mathbf{N_c-2}} & \mathbf{H}_{\mathbf{k,j,N_c-1}}^{\mathbf{N_c-1}} \end{bmatrix}$$

$$, \quad \ldots\ldots \textbf{(29)}$$

Here, $H_{k,j}^{1} = [H_{k,j,0}^{1} \cdots H_{k,j,N_c-1}^{1}]^T$ and $H_{k,j}^{N_c-1} = [H_{k,j,0}^{N_c-1} \cdots H_{k,j,N_c-1}^{N_c-1}]^T$ need to be calculated. In the 2^{nd} iteration, $H_{k,j}^{2} = [H_{k,j,0}^{2} \cdots H_{k,j,N_c-1}^{2}]^T$ and $H_{k,j}^{N_c-2} = [H_{k,j,0}^{N_c-2} \cdots H_{k,j,N_c-1}^{N_c-2}]^T$need to be calculated

and so forth. Two more columns of the matrix are calculated at every iteration and two more interfering subcarriers are cancelled at each iteration. At last, the ICI cleaned signal $Y_{k,n}^{(t)}$ is fed forward to the MPD.

The proposed algorithm can suppress multiple-antenna interferences and cancel inter-carrier interferences iteratively and progressively until a stopping criterion is satisfied. The estimated soft data symbols are calculated using below equation for QPSK or 16-QAM:

$$: \hat{S}_{j,n}^{(t)} = \frac{1}{\sqrt{2}} \cdot \tilde{b}_{mj,n} + j\frac{1}{\sqrt{2}} \cdot \tilde{b}_{mj+1,n}, \quad \ldots..\textbf{(30)}$$

$$: \hat{S}_{j,n}^{(t)} = -\frac{1}{\sqrt{10}} \cdot \tilde{b}_{mj,n} \cdot (2 + \tilde{b}_{mj+2,n}) - j\frac{1}{\sqrt{10}} \cdot \tilde{b}_{mj+1,n} \cdot (2 + \tilde{b}_{mj+3,n})$$

$$, \quad \ldots..\textbf{(31)}$$

Where the soft bit information are obtained from MPD.

V. Simulation Results

An MIMO-OFDM model for simulations is constructed and its key parameters are listed. Throughout all simulations, the total average power of transmit antennas is set to 1. Thus the average power at each antenna is of 1 I Nt . In the simulations, the CFO is assumed to be smaller than the subcarrier spacing of OFDM, i.e., a fractional or residual CFO A. Precoding for PAPR Reduction Fig. 1 illustrates the complementary cumulative distribution function of the PAPR for the precoded MIMOOFDM signals for different beta values (roll-off rates). It is observed that the proposed precoding scheme provides considerable gains in PAPR reduction for 2x2 MIMOOFDM signals compared to that of original MIMO-OFDM. The PAPR value is reduced with the increase of beta. Note that a raise of beta also results in an increase in the number of subcarriers and computational cost.

Let the true CFO be randomly chosen from the range [-0.2, 0.2]. The initial value & (0) is set equal to the boundary value, either -0.2 or +0.2. The mean square error (MSE) versus EM iterations for 2x2 MIMO-OFDM is shown in Fig. 2. Note that the MSE curves corresponding to different SNRs are similar before 10 iterations. In particular, the MSE curve with SNR 5dB converges to 0.2xlO-4 after 18 iterations. For the SNR higher than 15dB, the MSE perfonnance converges to 10-6 after 23 iterations.

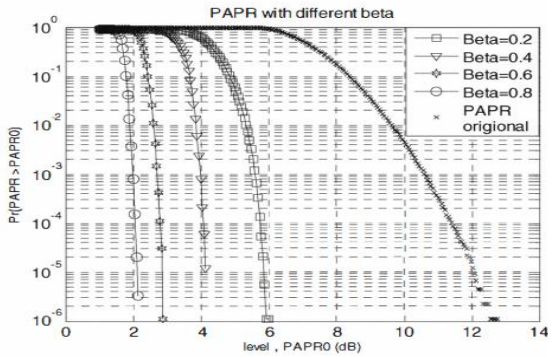

Fig:3 PAPR reduction of 2x2 MIMO-OFDM for various beta values.

The BER performance of the proposed message passing algorithm on factor graph for data detection/decoding and ICI cancellation in bit-interleaved LDPC-coded MIMO-OFDM systems are simulated with $Nt = Nr = 2$ and QPSK modulation. Gallager code with codeword length 20 is used. The dimension of the parity check matrix of Gallager code is 15×20 with row weight $dc = 4$ and column weight $dv = 3$. The FFT size of OFDM modulator is 1024. A S-random interleaver of length 8192, $S = 64$ is used after the LDPC

encoding. The multipath channel model is the ITU vehicular A channel. The fading channel model used is the Jakes' model [9].

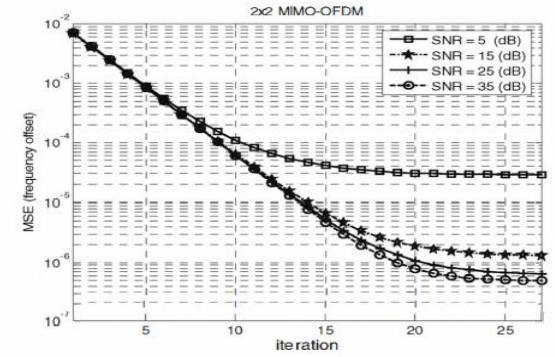

Fig: 4 MSE Vs Iteration for 2x2 MIMO-OFDM with various SNR values.

In the case of imperfect channel estimation, two different models are used to model the variance of channel estimation error: a) $\sigma 2E$is independent of the SNR.b) $\sigma 2E$is a decreasing function of SNR. The carrier frequency is 2.5 GHz, bandwidth is 10 MHz, sampling frequency is 11.2 MHz, subcarrier spacing is 10.93 kHz, useful OFDM symbol duration is 91.43 μs and the length of cyclic prefix is 1/8 [10]. The vehicular speeds are 350 km/h which are corresponding to maximum Doppler frequency 810 Hz and normalized Doppler frequency 0.07.

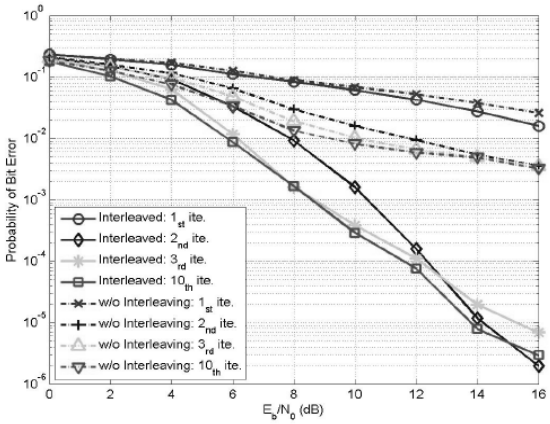

Fig: 5 with interleaving Vs without interleaving

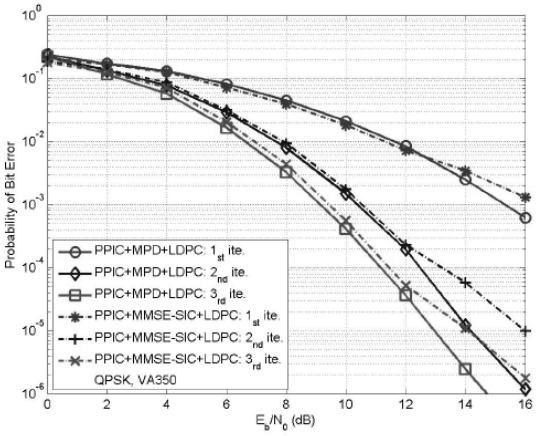

Fig: 6 Performance comparisons of message passing MIMO detector and MMSE-SIC MIMO detector

VI. Conclusions

This paper proposed an iterative scheme based on the EM algorithm for joint estimation of the CFO and CIR of the MIMO-OFDM system with the PAPR reduction precoder. A minimum error probability based precoding matrix to reduce the PAPR of OFDM signals was designed. The problem of estimating the frequency offset and channel parameters in MIMO-OFDM system with the PAPR reduction precoding scheme is investigated. To reduce computational complexity, a simple CFO estimator is derived in the coarse estimation phase and the resulted estimate is used in the fine estimation phase. Hence a more accurate estimate can be achieved at a less number of iterations. Simulation results show that the CFO estimator with a coarse initial estimate not only has an excellent performance at reduced computational complexity, but also makes the CIR estimator achieve almost ideal performance. Based on factor graph, a joint design of message passing MIMO data detector/decoder with PPIC ICI canceller for OFDM-based wireless communication systems is proposed. The proposed algorithm can suppress inter-antenna interferences in space domain and cancel inter-carrier interferences in frequency domain iteratively and progressively. With a proper designed message passing schedule and random interleaver, the short cycle problem is solved.

References

[1] E. Biglieri, A. Nordio, and G. Taricco, "EXIT-chart analysis of iterative MIMO interfaces," *ISITA2004*, Oct. 2004.

[2] A. D. Kora, A. Saemi, J. P. Cances, and V. Meghdadi, "New list sphere decoding (LSD) and iterative synchronization algorithms for MIMOOFDM detection with LDPC FEC," *IEEE Trans. Veh. Technol.*, vol. 57, no. 6, pp. 3510-3524, Nov. 2008.

[3] L. Ben, G. Yue, and X. Wang, "Performance analysis and design optimization of LDPC-coded MIMO OFDM systems," *IEEE Trans. Signal Process.*, vol. 52, no. 2, pp. 348-361, Feb. 2004.

[4] M. Russell and G. L. Stuber, "Interchannel interference analysis of OFDM in a mobile environment," in *Proc. IEEE VTC*, pp. 820-824, vol. 2, July 1995.

[5] K. Sathananthan and C. Tellambura, "Probability of error calculation of OFDM systems with frequency offset," *IEEE Trans. Commun.*, vol. 49, no. 11, pp. 1884-1888, Nov. 2001.

[6] T. Pollet, M. Van Bladel, and M. Moeneclaey, "BER sensitivity of OFDM systems to carrier frequency offset and Wiener phase noise," *IEEE Trans. Commun.*, vol. 43, no. 234, pp. 191-193, Feb.-Mar.-Apr. 1995.

[7] P. Robertson and S. Kaiser, "The effects of Doppler spreads in OFDM(A) mobile radio systems," in *Proc. IEEE VTC Fall*, vol. 1, pp. 329-333, Sep. 1999.

[8] Y. Li and L. J. Cimini, Jr., "Bounds on the interchannel interference of OFDM in time-varying impairments," *IEEE Trans. Commun.*, vol. 49, no. 3, pp. 401-404, Mar. 2001.

[9] Y. Zhao and S. G. Haggman, "Intercarrier interference self-cancellation scheme for OFDM mobile communication systems," *IEEE Trans. Commun.*, vol. 49, no. 7, pp. 1185-1191, July 2001.

[10] Y. Wang, S. Zhu. and Y. Li, "A method to improve the bandwidth efficiency of self ICI cancellation in OFDM systems," in *Proc. International Conf. Signal Process.*, vol. 2, pp. 1633-1636, 2002.